Molecular structure of 1-(dichloroboryl)pentaborane(9), in the gas phase as determined by electron diffraction and supported by theoretical calculations

7 AUTHORS, INCLUDING:

Ian Alberts

City University of New York - LaGuardia Co…

51 PUBLICATIONS **1,227** CITATIONS

SEE PROFILE

Anthony J Downs

University of Oxford

258 PUBLICATIONS **5,062** CITATIONS

SEE PROFILE

Molecular Structure of 1-(Dichloroboryl)pentaborane(9), in the Gas Phase as determined by Electron Diffraction and supported by Theoretical Calculations

Paul T. Brain,[a] David W. H. Rankin,*,[a] Heather E. Robertson,[a] Ian L. Alberts,[a] Anthony J. Downs,[b] Tim M. Greene,[b] Matthias Hofmann[c] and Paul von Ragué Schleyer[c]

[a] Department of Chemistry, The University of Edinburgh, West Mains Road, Edinburgh EH9 3JJ, UK

[b] Inorganic Chemistry Laboratory, The University of Oxford, South Parks Road, Oxford OX1 3QR, UK

[c] Computer-Chemie-Centrum des Institut für Organische Chemie, Universität Erlangen–Nürnberg, Nägelbachstrasse 25, D-91052 Erlangen, Germany

The structure of gaseous 1-(dichloroboryl)pentaborane(9), 1-(Cl_2B)B_5H_8, has been determined by electron diffraction. The results confirm that the molecule consists of a pentaborane(9) cage substituted at the apical boron atom, B(1), by a dichloroboryl group; the BCl_2 moiety is essentially free to rotate about the exo B–B bond. Salient experimental structural parameters (r_a) are r(B–B) (base–base) 182.1(14), r(B–B) (base–apex) 173.9(26), r(B–B) (apex–exo) 170.1(18), r(B–Cl) 172.0(15), r(B–H_t) 126.2(22), and r(B–H_b) 134.6(16) pm (H_t = terminal hydrogen, H_b = bridging hydrogen); Cl–B–Cl 121.7(28)°, B–H_t 'rise' (above basal-boron plane) 15.1(26)°, and B–H_b 'dip' (below basal-boron plane) 62.0(39)°. These conclusions are supported by ab initio (MP2/6–31G* or MP2/DZP level) optimisations of the molecular geometry, and by comparison of the calculated ^{11}B NMR chemical shifts {individual gauge for localised orbitals (double zeta)//gas-phase electron diffraction level [IGLO(DZ)//GED level]} with the experimental NMR data.

Although compounds containing two-centre, two-electron B–B bonds have been known since Stock et al.[1] discovered B_2Cl_4 in 1925, it was not until 1982 that the first dihalogenoboryl boron hydride, 1-(Cl_2B)B_5H_8, was reported.[2] More recently, a new synthetic route to 1-(dihalogenoboryl)pentaborane(9) derivatives, 1-(X_2B)B_5H_8 (X = F, Cl, Br or I), has for the first time allowed preparation of these compounds in amounts which are commensurate with a thorough characterisation of their physical and chemical properties.[3,4]

With the exception of 1-(I_2B)B_5H_8,[4] all of the 1-(dihalogenoboryl)pentaborane(9) derivatives are volatile and thermally stable enough to be structurally characterised by gas-phase electron diffraction (GED).[2–4] We have reported the molecular structure of 1-(F_2B)B_5H_8 as determined by GED and ab initio computations.[5] The compound consists of a B_5H_8 cage of C_{4v} symmetry substituted at the apical boron by a BF_2 group which is free to rotate about the B–B (apex–exo) bond. We now extend this study to the chloro analogue, 1-(Cl_2B)B_5H_8.

The use of the combined ab initio/IGLO/NMR method[5–8] to augment and/or support the determination of gas-phase structures by electron diffraction has proved to be very successful, especially for relatively small boranes.[5,8b–d] In this approach, various structures derived from experiment and from ab initio geometry optimisations are assessed by means of IGLO (individual gauge for localised orbitals)[6] NMR calculations. The [11]B chemical shifts obtained by this method for various geometries are compared with the experimental chemical shifts. Using geometries optimised at electron-correlated levels of theory (e.g. MP2/6–31G*, i.e. with a basis set including polarisation functions) gives agreement between experimental and IGLO [11]B chemical shifts which has been found to be consistently good.[7a]

In electron-diffraction analyses the parameters defining the structures of boranes, especially those for the boron framework, are often subject to significant correlation.[5,8b–d] Moreover, it is possible that several geometries will fit the

electron-scattering data more or less equally well, and additional information (e.g. from spectroscopic or theoretical sources) is required to decide which of the options is correct.[9] Whenever it is feasible, therefore, we perform both experimental and theoretical work, so that the results obtained are as reliable as possible.

The electron-scattering pattern of 1-(Cl_2B)B_5H_8 has been analysed and the refined structure found to be in good agreement with the geometry obtained by the ab initio study. The reliability of the structure is further substantiated by ab initio energy and [11]B chemical-shift calculations.

Experimental

Synthesis.—1-(Dichloroboryl)pentaborane(9) was prepared using a method similar to that reported recently by Saulys and Morrison,[3] i.e. by the reaction of diboron tetrachloride, B_2Cl_4, with pentaborane(9).[4] The purity of the compound was checked by reference (i) to the IR spectrum of the vapour and that of a solid film at 77 K,[2,4] (ii) to the ^{1}H and ^{11}B NMR spectra of a [$^2H_8$] toluene solution,[2–4] and (iii) to the mass spectrum of the vapour.[2–4]

Electron-diffraction Measurements.—Electron-scattering measurements were recorded on Kodak Electron Image plates using the Edinburgh gas-diffraction apparatus operating at ca. 44.5 kV (electron wavelength ca. 5.7 pm).[10] Nozzle-to-plate distances were ca. 202 and 260 mm yielding data in the range s 20–216 nm^{-1}; two usable plates were obtained at each distance.

Owing to the reactivity of the compound, the use of the normal stainless-steel nozzle was considered to be undesirable. Instead, an all-glass inlet nozzle, designed originally for the diffraction of gallane,[11] was employed. This permitted the passage of the vapour into the diffraction chamber with exposure limited to preconditioned Pyrex-glass surfaces. Although it would have been desirable to hold the sample

and nozzle at *ca.* 273 K during the experiment to reduce the possibility of thermal decomposition,[2-4] it was found that this temperature gave a molecular flux insufficient to yield a diffraction pattern with an adequate signal-to-noise ratio. The sample and nozzle were therefore held at *ca.* 293 K during the exposure periods. Prior to the first exposure at each camera distance, the sample, held at *ca.* 293 K, was subjected briefly to pumping in order to condition all the surfaces exposed to the vapour, and also to remove any volatile decomposition products formed during storage and prior manipulation of the compound. The exposed plates were left *in vacuo.* for 24 h and washed before developing.

Scattering patterns of benzene were also recorded for the purpose of calibration; these were analysed in exactly the same way as those of the pentaborane(9) derivative so as to minimise systematic errors in the wavelengths and camera distances. Nozzle-to-plate distances, weighting functions used to set up the off-diagonal weight matrix, correlation parameters, final scale factors, and electron wavelengths for the measurements are collected together in Table 1.

The electron-scattering patterns were converted into digital form using a computer-controlled Joyce-Loebl MDM6 microdensitometer with a scanning program described elsewhere.[12] The programs used for data reduction[12] and least-squares refinement[13] have been described previously; the complex scattering factors employed were those listed by Ross *et al.*[14]

Theoretical Calculations.—The structure of 1-(dichloro-boryl)pentaborane(9) was optimised at the Hartree-Fock (HF) and MP2 levels of theory employing standard procedures for the GAUSSIAN 92 (Erlangen)[15] and CADPAC5 (Edin-burgh)[16] programs; 6–31G*, DZ and DZP basis sets were used to assess the effect of both electron correlation and polar-isation functions on the quality of such calculations.[17,18] Total electronic energies were also calculated; since it was not possible to optimise the structure using the TZ2P basis (through limitations of computing time), the geometries optimised at the MP2/DZP level were employed in these latter energy calculations. It has been shown elsewhere that the precision of theoretical geometrical parameters for such systems does not change significantly at computational levels above MP2/DZP, even when large basis sets such as TZ2P are used.[7a,19]

The ^{11}B NMR chemical shifts for 1-(Cl$_2$B)B$_5$H$_8$ were calculated using the IGLO method employing a Huzinaga basis set[20] of double zeta (DZ) quality.[6c] The theoretical chemical shifts have been referenced to BF$_3$•OEt$_2$, as described elsewhere,[7a] and are given in the notation 'level of the chemical shift calculation // geometry employed'.

Calculations were performed on the Convex C3840 and Cray YMP-8 facilities at the Rutherford-Appleton Laboratory (RAL) and the University of London Computing Centre (ULCC), the Convex C220 of the Computer-Chemie-Centrum der Universität Erlangen-Nürnberg and a Cray YMP-8 of the Leibniz Rechenzentrum in Munich.

Molecular Model

On the basis of the spectroscopic evidence,[2-4] the molecular

model used to generate the atomic coordinates of 1-(Cl$_2$B)B$_5$H$_8$ was identical to that used to determine the structure of 1-(F$_2$B)B$_5$H$_8$[5] except, of course, that the fluorine atoms bonded to the *exo* boron atom, B(6), were replaced by chlorine atoms. In the final refinements such a model was described by the parameters listed in Table 2; the atom numbering scheme is shown in Fig. 1.
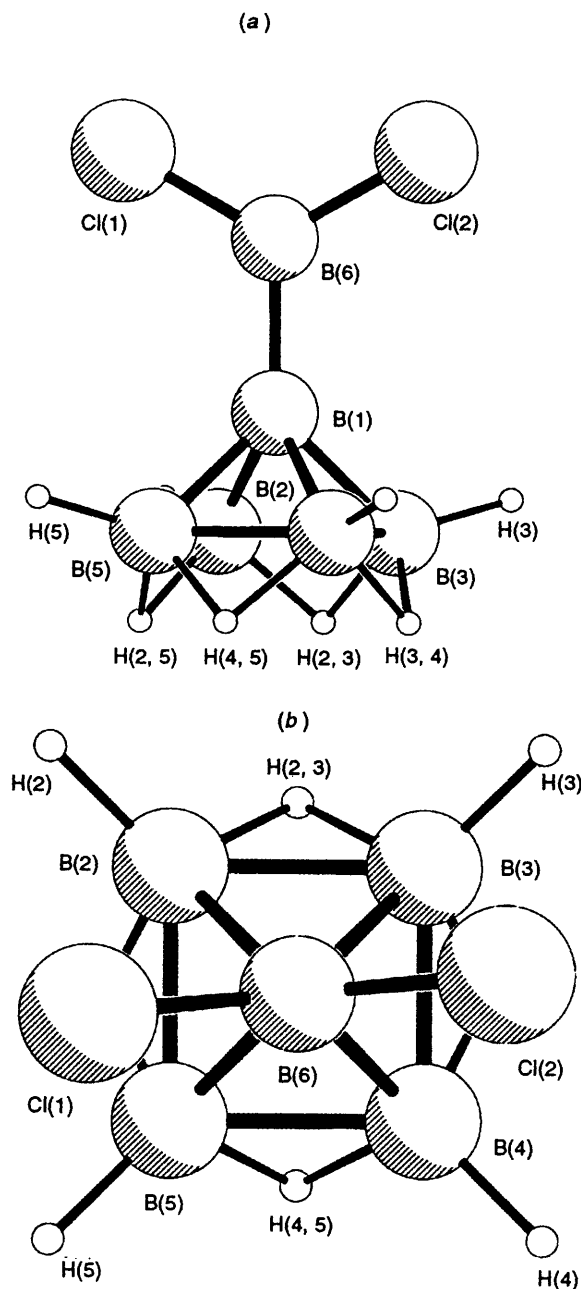

Fig. 1 Optimum experimental (GED) structure of 1-(Cl$_2$B)B$_5$H$_8$: (*a*) perspective view and (*b*) view along the B–B(*exo*-apex) bond

Table 1 Nozzle-to-plate distances, weighting functions, correlation parameters, scale factors and electron wavelengths

Nozzle-to-plate distance/mm	Δs	s_{min}	sw_1	sw_2	s_{max}	Correlation parameter	Scale factor, k^a	Electron wavelength[b]/pm
	nm^{-1}							
259.61	2	20	40	142	166	0.479	0.813(14)	5.671
201.65	4	40	60	184	216	0.222	0.848(18)	5.823

[a] Figures in parentheses are the estimated standard deviations. [b] Determined by reference to the scattering pattern of benzene vapour.

The Boron Cage.—The B_5H_8 cage was assumed to possess C_{4v} symmetry with one terminal hydrogen atom (H_t) associated with each basal boron atom and with four bridging hydrogen atoms (H_b), each equidistant from two basal boron atoms. The cage structure was then defined by two different B–B interatomic distances (base–base and base–apex), two B–H interatomic distances (terminal and bridging), and two angles defining the orientation of the B–H_t and B–H_b–B units. These angles were chosen to be measured relative to the basal plane of the B_5 pyramid, upwards (towards the apex) for the B–H_t unit ('H_t rise') and downwards (away from the apex) for the B–H_b–B unit ('H_b dip').

The Chloroboryl Group.—The B–BCl_2 moiety, with local C_{2v} symmetry (C_2 axis coincident with the C_4 axis of the boron cage), was defined by four parameters: the B–B (apex-*exo*) and the B–Cl distances, the Cl–B–Cl angle, and a parameter defining the location of the chlorine atoms relative to the basal boron and the hydrogen atoms. In the initial refinements this parameter was defined as a torsion angle allowing the BCl_2 group to twist about the B–B (*apex–exo*) bond, such that the plane of the BCl_2 unit did not necessarily contain two of the bridging hydrogen atoms (torsion angle = 0°) but could take up an orientation between the two different types of hydrogen atom when viewed along the B–B (*exo*-apex) axis [see Fig. 1(*b*)]. In the later refinements, however, it was replaced by a parameter which was defined as a potential-energy barrier to rotation (V_0) of the BCl_2 moiety about the B–B (apex–*exo*) bond. This was achieved by representing the rotation as a set of four fixed conformations of the BCl_2 group over the range $0 \leqslant \varphi \leqslant 45°$ of the rotation angle, φ ($\varphi = 0°$ being defined as where the two bridging hydrogens are in the BCl_2 plane). Thus, the continuous torsion-sensitive distance distribution was approximated by calculating the non-bonding distances $r(\text{Cl} \cdots \text{B})$ and $r(\text{Cl} \cdots \text{H})$ at angle increments $\Delta\varphi = 11.25°$; 48 distinct torsion-sensitive distances were generated by this scheme. The low-barrier classical approximation (1) for the probability

$$P(\varphi) = N\{\exp[-V(\varphi)/RT]\} \qquad (1)$$

distribution of the rotation angle (φ) was adopted and the potential function assumed to be of the form (2). The relative

$$V(\varphi) = (V_0/2)(1 - \cos 4\varphi) \qquad (2)$$

multiplicities of the 16 $r(\text{Cl} \cdots \text{B})$ and the 32 $r(\text{Cl} \cdots \text{H})$ distinct non-bonded distances were each weighted according to $P(\varphi)$. The overall structure, with C_{2v} symmetry for a 0 or 45° rotation of the BCl_2 group, was then defined by 10 independent parameters.

Refinement of the Structure

The radial-distribution curve for 1-$(Cl_2B)B_5H_8$ (Fig. 2) shows four peaks at distances shorter than 340 pm; these occur near 129, 175, 261 and 300 pm. The peaks at $r < 200$ pm correspond to scattering from bonded atom pairs; the terminal and bridging B–H distances constitute the peak at 129 pm, whereas the most intense peak at 175 pm has contributions from the B–Cl and the three different B–B bonded distances. The two-bond B $\cdots$ H non-bonded pairs are identified with the peak at 261 pm, augmented by the B $\cdots$ B (base $\cdots$ base) pair, whilst the feature at 300 pm is attributed to the B(apex) $\cdots$ Cl, the B $\cdots$ B (base $\cdots$ *exo*) and the Cl $\cdots$ Cl non-bonded pairs. The radial-distribution curve at $r > 340$ pm consists of several broad features encompassing the B(base) $\cdots$ Cl and H $\cdots$ Cl non-bonded distances in the molecule.

Initial refinements of the molecular structure employing a static model, *i.e.* incorporating p_{10} as a BCl_2 'twist angle', yielded parameters similar to those reported in Table 2, with $p_{10} = 23.3(8)°$. However, the potential-energy (p.e.) difference between the conformation in which the chlorine atoms eclipse the bridging hydrogen atoms (p.e. minima) and that in which they eclipse the terminal hydrogen atoms (p.e. maxima) calculated *ab initio* (*ca.* 0.92 kJ mol^{-1} at the MP2/TZ2P level, see
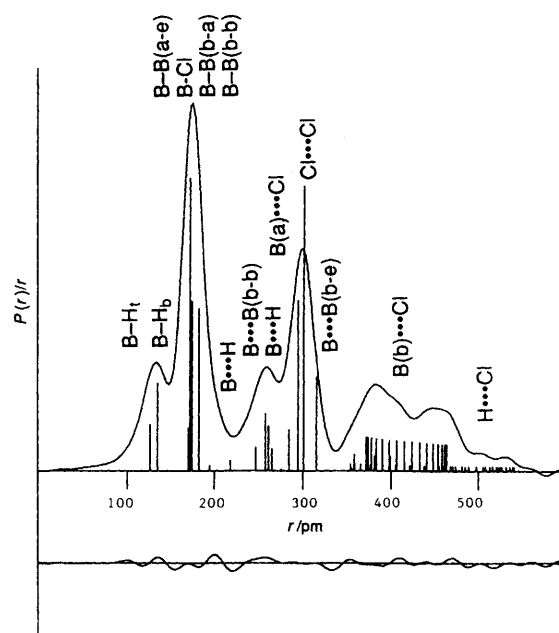

Fig. 2 Observed and final weighted radial-distribution curves for 1-$(Cl_2B)B_5H_8$. Before Fourier inversion, the data were multiplied by $s \cdot \exp[(-0.000\ 03s^2)/(Z_B - f_B)(Z_{Cl} - f_{Cl})]$. Notation in parentheses: a = apex, b = base, e = *exo*

Table 2 Structural parameters for 1-$(Cl_2B)B_5H_8$ (distances/pm, angles/°, V_0/kJ mol^{-1})

Parameter[a]	Electron diffraction[b] (r_a)	Theoretical[c] (r_e)
p_1 r(B–B) (base–base)	182.1(14)	179.6/177.8
p_2 r(B–B) (base–apex)	173.9(26)	169.0
p_3 r(B–B) (apex-*exo*)	170.1(18)	166.1
p_4 r(B–Cl)	172.0(15)	175.6
p_5 r(B–H) (terminal)	126.2(22)	118.6
p_6 r(B–H) (bridge)	134.6(16)	134.2/134.3
p_7 Cl–B–Cl	121.7(28)	117.0
p_8 B–H_t 'rise' (above basal plane)	15.1(26)	7.4
p_9 B–H_b 'dip' (below basal plane)	62.0(39)	62.7/63.7
p_{10} Barrier to BCl_2 rotation, V_0	0.0(10)	0.59[d]

[a] For definitions of parameters, see the text. Figures in parentheses are the estimated standard deviations. [b] Electron diffraction of the vapour assuming free rotation of the BCl_2 group. [c] Optimised geometry at the MP2(fc)/6–31G* level based on a 0° BCl_2 twist (Cl atoms lying above H_b). [d] $V_0 = E$(geometry with BCl_2 twist angle = 45°) − E(geometry with BCl_2 twist angle = 0°). Calculated at the MP2(fc)/6–31G* level.

Table 3 Least-squares correlation matrix (× 100) for 1-$(Cl_2B)B_5H_8$*

p_2	p_3	p_4	p_5	p_6	p_7	p_9	u_1	u_8	
-52	78			54		77	-66	51	p_1
		-88	63	-60	95			-96	p_2
						53	-53		p_3
			-56		-97			87	p_4
				-63	63			-55	p_5
					-55	50		53	p_6
								-94	p_7
							-58		p_9

* Only elements with absolute values ⩾50% are shown.

below) was indicative of a structure in which the barrier to rotation of the BCl_2 moiety about the B–B(apex–exo) bond is low, relative to RT. In subsequent refinements a dynamic model, incorporating p_{10} as the potential-energy barrier V_0 as described above, was employed.

All nine of the independent parameters defining the molecular geometry refined simultaneously. The parameters relating to the heavy-atom skeleton (p_1–p_4 and p_7) were correlated significantly, because the respective B–B and B–Cl bonded distances all lie under the same peak in the radial-distribution curve. As a result, the estimated standard deviations (e.s.d.s) for these parameters are relatively large compared with analogous values for 1-$(F_2B)B_5H_8$.[5] The starting values for the amplitudes of vibration (u) were derived from the ab initio force field, computed at the MP2/6–31G* level, using the program ASYM20.[21] It was possible to refine three groups of amplitudes in the final refinement, the ratios within these groups being maintained at the values derived from the ab initio force field.

It was not possible to refine the potential-energy barrier, p_{10}, freely. Its value in the final refinement was determined by plotting R_G vs. p_{10} for a series of refinements in which p_{10} was varied stepwise such that $-6.0 \leqslant p_{10} \leqslant 6.0$ kJ mol^{-1}. The resultant function was approximately quadratic in p_{10}, giving $p_{10} = 0.0(20)$ kJ mol^{-1} at the 95% confidence level,[22] implying an e.s.d. of 1.0 kJ mol^{-1}.

The success of the final refinement, for which $R_G = 0.102$ ($R_D = 0.075$), may be assessed on the basis of the difference between the experimental and calculated radial-distribution curves (Fig. 2). Fig. 3 offers a similar comparison between the experimental and calculated molecular-scattering curves, whilst the most significant values of the least-squares correlation matrix are shown in Table 3. The interatomic distances and vibrational amplitudes of the optimum refinement are listed in Table 4, atomic coordinates in Table 5.

Ab Initio Calculations

Two conformational stationary points were located on the ground-state potential-energy surface of 1-$(Cl_2B)B_5H_8$; these correspond to twist angles of 0 (two H_b atoms in the BCl_2 plane, conformation 1) and 45° (two H_t atoms in the BCl_2 plane, conformation 2) of the BCl_2 group about the B–B (apex–exo) bond. The calculated geometrical parameters for the two conformations are very similar and are presented in Table 6. Energetically, conformation 1 was calculated consistently to be favoured over conformation 2 (see below); conformation 2 corresponds to a transition state for the BCl_2 rotation (one imaginary frequency of -13.4 cm^{-1} at the RHF/6–31G* level).

Discussion

Analysis of the gas-phase electron-diffraction pattern and ab initio optimisation of the geometry endorse the spectroscopic evidence that the 1-(dichloroboryl)pentaborane(9) molecule consists of a square-pyramidal B_5H_8 cage with a BCl_2 group σ-bonded to the apical B(1) atom. As with 1-$(F_2B)B_5H_8$,[5]
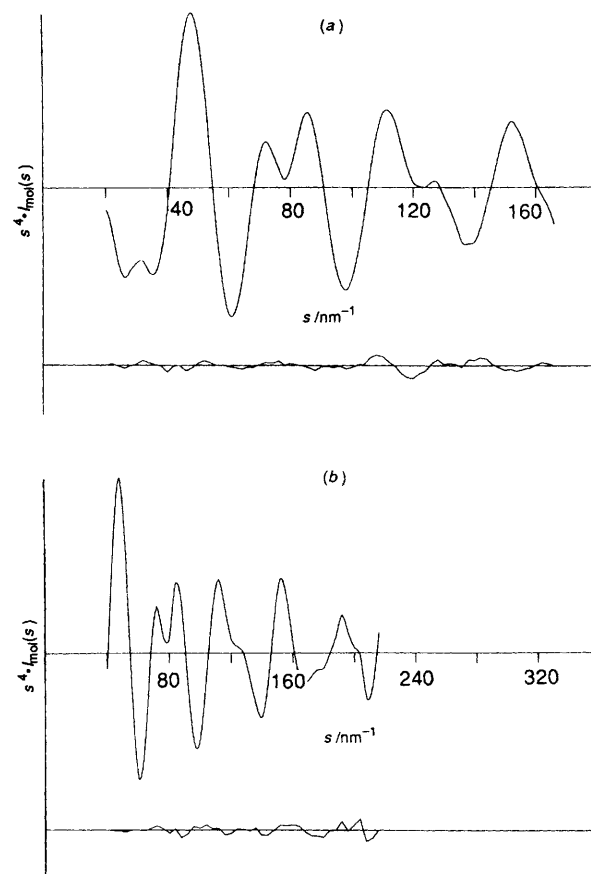
Fig. 3 Observed and final weighted difference molecular-scattering intensity curves for 1-$(Cl_2B)B_5H_8$. Nozzle-to-plate distances were (a) 259.6 and (b) 201.7 mm

the dihalogenoboryl group is found to be essentially free to rotate about the B–B (apex–exo) bond.

With due allowance for the relatively large e.s.d.s attaching to the experimental results, the parameters derived by the ab initio calculations for 1-$(Cl_2B)B_5H_8$ (Table 6) are in reasonably good agreement with those refined on the basis of the electron-diffraction pattern (Table 2). In particular, the predicted B–B bond lengths are in the correct order with r(B–B) (base–base) > r(B–B) (base–apex) > r(B–B) (apex–exo). It is clear from Table 6 that both electron-correlation and polarisation functions must be included in the theoretical calculations for reliable results to be obtained. Thus, at the MP2/DZP or MP2/6–31G* levels, the theoretical paramaters offer good support for those derived experimentally.† The predicted value

† It should be borne in mind, however, that this procedure involves comparison of two different structure types, namely r_a (from GED) and r_e (from calculations).[23]

of V_0 (corresponding to the BCl_2 rotational barrier) ranges from 2.09 (MP2/DZ level) to 0.59 kJ mol^{-1} (MP2/6–31G* level) for methods including electron correlation (Table 6); at the MP2/TZ2P//MP2/DZP level, the highest available to us, the final value of V_0 is 0.92 kJ mol^{-1}. In the gas phase at 293 K,

Table 4 Interatomic distances (r_a/pm) and amplitudes of vibration (u/pm) for 1-$(Cl_2B)B_5H_8$ [a]

		Distance	Amplitude [b]	
r_1	B(2)–B(3)	182.1(14)	6.9(5)	
r_2	B(1)–B(2)	173.9(26)	6.6	⎫
r_3	B(1)–B(6)	170.1(18)	5.9	⎬ (tied to u_1)
r_4	B(6)–Cl(1)	172.0(15)	5.5	⎭
r_5	B(2)–H(2)	126.2(22)	8.5(f)	
r_6	B(2)–H(2,3)	134.6(16)	11.2(f)	
r_7	B(2)···B(4)	257.5(19)	6.5(f)	
r_8	B(2)···B(6)	314.5(33)	11.0(18)	
r_9	B(1)···Cl(1)	295.0(39)	9.0	⎫ (tied to u_8)
r_{10}	Cl(1)···Cl(2)	300.4(17)	7.8	⎬
r_{11}	B(2)···H(3)	283.7(20)	11.8	⎫
r_{12}	B(2)···H(3,4)	261.2(31)	12.6	⎬ (f)
r_{13}	B(1)···H(4)	264.4(43)	11.7	⎭
r_{14}	B(1)···H(3,4)	246.3(32)	10.8	⎫
r_{15}	B(2)···H(4)	380.8(25)	10.2	⎬
r_{16}	B(6)···H(3,4)	398.9(31)	12.6	⎬ (f)
r_{17}	B(6)···H(4)	356.9(66)	19.6	⎭
r_{18}	B(2)···Cl(1)	389.9(11)		⎫
r_{19}	B(3)···Cl(1)	454.4(7)		⎬ 14.0(11)
r_{20}	B(4)···Cl(1)	448.5(8)		⎭
r_{21}	B(5)···Cl(1)	383.0(12)		⎫
r_{22}	Cl(1)···H(4)	497.3(48)		
r_{23}	Cl(1)···H(3,4)	540.9(22)		
r_{24}	Cl(1)···H(3)	507.7(48)		
r_{25}	Cl(1)···H(2,3)	505.5(26)		⎬ 15.1(rf)
r_{26}	Cl(1)···H(2)	389.6(51)		
r_{27}	Cl(1)···H(2,5)	458.6(42)		
r_{28}	Cl(1)···H(5)	376.0(52)		
r_{29}	Cl(1)···H(4,5)	497.4(28)		⎭
r_{30}	H(2,3)···H(3,4)	194.6(75)	16.1	⎫
r_{31}	H(2)···H(2,3)	217.8(37)	15.0	
r_{32}	H(2,5)···H(3,4)	275.2(106)	19.0	⎬ (f)
r_{33}	H(2)···H(3)	354.5(34)	18.1	
r_{34}	H(2)···H(3,4)	380.8(35)	15.1	
r_{35}	H(2)···H(4)	501.3(48)	12.9	⎭

[a] For atom numbering scheme see Fig. 1. Figures in parentheses are the estimated standard deviations. Additional 12 B···Cl and 24 Cl···H non-bonded distances were also included in the refinements, but are not listed here. These spanned the ranges 371.6(13)–463.8(7) pm and 353.0(54)–539.5(22) pm, respectively. [b] rf = Refined then fixed, f = fixed. Unrefined amplitudes were fixed at values calculated using the MP2/6–31G* force field.

$RT = ca.$ 2.4 kJ mol^{-1} and sufficient thermal energy is present to overcome the calculated small barrier; therefore, free rotation is the predicted experimental observation.

Further evidence for the reliability of the electron-diffraction structure comes from the calculation of the $\delta(^{11}B)$ and relative energy values (Table 7). These have been computed for the theoretically optimised equilibrium ($\varphi = 0°$) and transition-state geometries ($\varphi = 45°$), and for two of the conformations used in the dynamic electron-diffraction model, viz. $\varphi = 5.6$ and 39.4°. The IGLO ^{11}B chemical shifts show reasonable agreement with the experimental values and the GED geometries are computed (MP2/6–31G* single-point) to lie about 55 kJ mol^{-1} higher in energy than the respective fully optimised theoretical structure. Such an 'excess energy' is consistent with the range found for similar boranes and carbaboranes.[5,7a,8b–d] In addition, partial optimisations of the two electron-diffraction conformations were also undertaken; here the heavy-atom skeleton remained fixed but the locations of the hydrogen atoms varied.[24] These so-called 'hydrogen-relaxed' GED geometries of 1-$(Cl_2B)B_5H_8$ optimised to structures with calculated energies only 14.2 and 11.5 kJ mol^{-1} ($\varphi = 5.6$ and 39.4°, respectively) greater than those for the fully optimised theoretical structure. Thus, the majority of the 'excess energy' calculated for the experimental structure is attributable to the positions of the hydrogen atoms, which are poorly determined in the electron-diffraction experiment.

It is noteworthy that all of the IGLO $\delta(^{11}B)$ calculations, irrespective of geometry, predict a shift for the exo-boron atom 4.4–5.9 ppm to high frequency of the experimentally observed value. In contrast, the corresponding maximum difference for 1-$(F_2B)B_5H_8$ was -2.7 ppm, i.e. to lower frequency.[5] A similar observation was made recently for B_2F_4 and B_2Cl_4.[25] Here, it was possible to allow for the effects of electron correlation (GIAO-MP2/TZP level) in computing the ^{11}B chemical shifts for the two diboron tetrahalides. The change in the values was insignificant (differences of 2.8 and 5.5 ppm, respectively), as it was on averaging the computed values for the staggered and planar conformations of each, and it is therefore unlikely that the discrepancy for 1-$(Cl_2B)B_5H_8$ can be attributed to neglect of electron correlation in the IGLO calculations.

A comparison of bond lengths for some pentaborane(9) derivatives and some boron chlorides is given in Table 8. Relative to B_5H_9,[26] the B_5 cages of the 1-$(X_2B)B_5H_8$ molecules (X = F or Cl) have expanded; both the experimental and theoretical $r(B–B)$ cage distances are greater for the 1-dihalogenoboryl derivatives. This is consistent with increased electron demand for σ B–B versus exo-terminal B–H bond formation. The $r(B–B)$ (apex–exo) distance in 1-$(Cl_2B)B_5H_8$ falls within the normal range found for two-centre, two-electron B–B bonds; other examples include: 2,2′-$(B_{10}H_{13})_2$,

Table 5 Atomic coordinates (pm) for 1-$(Cl_2B)B_5H_8$ [a]

	Electron-diffraction refinement			Ab initio optimisation		
Atom [b]	x	y	z	x	y	z
B(1)	0.0	0.0	116.9	0.0	0.0	112.2
B(3)/B(2)	±91.1	91.1	0.0	±88.9	89.8	0.0
B(4)/B(5)	±91.1	−91.1	0.0	±88.9	−89.8	0.0
B(6)	0.0	0.0	286.9	0.0	0.0	278.3
H(2)/H(5)	−177.2	±177.2	32.8	−172.1	±173.0	15.3
H(3)/H(4)	177.2	±177.2	32.8	172.1	±173.0	15.3
H(2,3)/H(4,5)	0.0	±137.6	−87.5	0.0	±134.5	−90.2
H(3,4)/H(2,5)	±137.6	0.0	−87.5	±134.7	0.0	−88.6
Cl(2)/Cl(1)	±149.5	±14.7	370.7	±149.7	0.0	370.0
Cl(2′)/Cl(1′)	±143.7	±43.6	370.7			
Cl(2″)/Cl(1″)	±132.5	±70.8	370.7			
Cl(2‴)/Cl(1‴)	±116.1	±95.3	370.7			

[a] For atom numbering scheme see Fig. 1. [b] Cl(1′), Cl(1″), Cl(1‴), etc., define the conformations used in the 'dynamic' electron-diffraction model. See the text.

Table 6 Theoretical structural parameters for 1-(Cl$_2$B)B$_5$H$_8$ (distances/pm, angles/°, V_0/kJ mol^{-1})

Parameter[a]	φ[b]/°	HF/DZ	MP2/DZ	HF/DZP	MP2/DZP	MP2/6–31G*
				Level of theory/basis set		
p_1 r(B–B) (base–base)	0	186.5/184.1	186.8/184.4	183.3/181.3	180.9/179.0	179.6/177.8
	45	185.3	185.6	182.3	179.9	178.7
p_2 r(B–B) (base–apex)	0	172.3	173.7	171.3	169.8	169.0
	45	173.2/171.5	174.8/172.8	172.0/170.6	170.6/169.1	169.7/168.4
p_3 r(B–B) (apex–*exo*)	0	165.7	165.9	168.1	165.8	166.1
	45	165.8	166.1	168.2	166.0	166.2
p_4 r(B–Cl)	0	183.4	184.6	177.2	175.1	175.6
	45	183.4	184.6	177.2	175.1	175.6
p_5 r(B–H) (terminal)	0	117.0	118.4	117.7	117.7	118.6
	45	117.0/117.0	118.5/118.4	117.7/117.7	117.7/117.7	118.7/118.6
p_6 r(B–H) (bridge)	0	136.7/136.7	137.8/137.8	135.3/135.2	134.5/134.3	134.3/134.2
	45	135.8/137.7	136.7/139.0	134.6/135.9	133.6/135.2	133.6/135.0
p_7 Cl–B–Cl	0	115.0	115.9	116.1	117.7	117.0
	45	114.9	115.8	116.0	117.5	116.9
p_8 B–H$_t$ 'rise'	0	11.3	11.1	10.0	10.0	7.4
	45	12.2/10.4	12.2/9.8	10.6/9.3	10.7/9.2	8.5/6.8
p_9 B–H$_b$ 'dip'	0	62.6/61.8	63.2/62.2	63.0/62.2	63.6/62.8	63.7/62.7
	45	61.6	62.0	62.2	62.7	62.8
p_{10} V_0^c	—	1.68	2.09	1.30	1.84	0.59

[a] For definitions of parameters, see the text. [b] φ = Angle of rotation of the BCl$_2$ group (φ = 0° defined as where two bridging hydrogens are in the BCl$_2$ plane). [c] V_0 = E(BCl$_2$ twist angle = 45°) − E(BCl$_2$ twist angle = 0°). At our highest attainable level, MP2/TZ2P//MP2/DZP, V_0 = 0.92 kJ mol^{-1}.

Table 7 IGLO Results for 1-(Cl$_2$B)B$_5$H$_8$

Level of theory//geometry (φ/°)	δ(^{11}B)[a]			Relative energy/kJ mol^{-1}
	B(apical)	B(basal)	B(*exo*)	
DZ//MP2/6–31G* (0)[b]	−54.7	−10.9	81.5	0.0
DZ//MP2/6–31G* (45)[c]	−54.8	−11.1	81.6	0.6
DZ//GED (5.6)	−49.0	−5.2	80.1	55.2
DZ//GED (H relaxed) (5.6)[d]	−53.0	−9.6	80.0	14.2
DZ//GED (39.4)	−49.1	−5.2	80.0	55.9
DZ//GED (H relaxed) (39.4)[d]	−53.3	−10.2	80.0	11.5
Experimental[e]	−52.2	−13.1	75.6	

[a] Relative to BF$_3$·OEt$_2$. [b] Chlorine atoms located above bridging hydrogens. [c] Chlorine atoms located above terminal hydrogens. [d] Hydrogen-atom positions optimised at the MP2/6–31G* level whilst holding heavy-atom skeleton at GED geometry. [e] This work. Recorded at 96.3 MHz in [^{2}H$_8$]toluene at 293 K.

Table 8 Bond lengths (pm) in some boron hydrides and their halogeno derivatives[a]

Molecule	Technique[b]	r(B–B)(base–base)	r(B–B)(base–apex)	r(B–B)(apex–*exo*)	r(B–Cl)	Ref.
B$_5$H$_9$	ED	181.1(4)	169.4(4)	—	—	26
	MP2	178.3	168.5	—	—	7(a)
1-(F$_2$B)B$_5$H$_8$	ED	181.2(6)	170.6(4)	167.6(7)	—	5
	MP2	179.3/178.0	169.0	167.1	—	5
1-(Cl$_2$B)B$_5$H$_8$	ED	182.1(14)	173.9(26)	170.1(18)	172.0(15)	This work
	MP2	179.6/177.8	169.0	166.1	175.6	This work
1,2′-(B$_5$H$_8$)$_2$	XRD	180.1(11)[c]	168.9(10)[c]	166.0(8)	—	30
BCl$_3$	ED	—	—	—	174.2(4)	27
	MP2	—	—	—	173.7	31
B$_2$Cl$_4$	ED	—	—	170.2(35)	175.0(6)	28
	MP2	—	—	168.8	173.8	25
B$_4$Cl$_4$	ED	170.3(11)	170.3(11)	—	169.3(8)	29
	MP2	169.0	169.0	—	172.1	25

[a] Figures in parentheses are the estimated standard deviations. [b] ED = Electron diffraction of the vapour, XRD = X-ray diffraction of a single crystal, MP2 = theoretical geometry optimised at the MP2/6–31G* level. [c] Mean value.

r = 169.2(3) pm;[32] 2,2′-(1-B$_9$H$_8$S)$_2$, r = 167.8(5) pm;[33] 3′,2-(2′,4′-C$_2$B$_5$H$_6$) [1,8,5,6-(η-C$_5$H$_5$)$_2$Co$_2$C$_2$B$_5$H$_6$], r = 165.4(8) pm;[34] and B$_2$(OMe)$_4$, r = 172.0(6) pm.[35] At 172.0(15) pm (MP2/6–31G*, 175.6 pm), the refined GED value of r(B–Cl) in 1-(Cl$_2$B)B$_5$H$_8$ is typical of other boron chlorides for which π-type interactions are thought to contribute significantly to the B–Cl bonding.[27–29]

Acknowledgements

References

1 A. Stock, A. Brandt and H. Fischer, *Ber. Dtsch. Chem. Ges.*, 1925, **58**, 855.

2 D. F. Gaines, J. A. Heppert, D. E. Coons and M. W. Jorgenson, *Inorg. Chem.*, 1982, **21**, 3662.

3 D. A. Saulys and J. A. Morrison, *Inorg. Chem.*, 1990, **29**, 4174.

4 P. T. Brain, D. Phil. Thesis, Oxford University, 1991.

5 P. T. Brain, D. W. H. Rankin, H. E. Robertson, I. L. Alberts, M. Hofmann and P. v. R. Schleyer, *Inorg. Chem.*, 1994, **33**, 2565.

6 (a) W. Kutzelnigg, *Isr. J. Chem.*, 1980, **19**, 193; (b) M. Schindler and W. Kutzelnigg, *J. Chem. Phys.*, 1982, **76**, 1919; (c) W. Kutzelnigg, U. Fleischer and M. Schindler, in *NMR, Basic Principles and Progress*, Springer, Berlin and New York, 1990, vol. 23, p. 165; (d) U. Meier, Ch. van Wüllen and M. Schindler, *J. Comput. Chem.*, 1992, **13**, 551.

7 (a) M. Bühl and P. v. R. Schleyer, *J. Am. Chem. Soc.*, 1992, **114**, 477; (b) M. Bühl and P. v. R. Schleyer, in *Electron Deficient Boron and Carbon Clusters*, eds. G. A. Olah, K. Wade and R. E. Williams, Wiley, New York, 1991, p. 113.

8 (a) D. Hnyk, E. Vajda, M. Bühl and P. v. R. Schleyer, *Inorg. Chem.*, 1992, **31**, 2464; (b) P. T. Brain, D. Hnyk, D. W. H. Rankin, M. Bühl and P. v. R. Schleyer, *Polyhedron*, 1994, **13**, 1453; (c) D. Hnyk, P. T. Brain, D. W. H. Rankin, H. E. Robertson, R. Greatrex, N. N. Greenwood, M. Bühl and P. v. R. Schleyer, *Inorg. Chem.*, 1994, **33**, 2572; (d) P. T. Brain, M. A. Fox, R. Greatrex, E. Leuschner, M. J. Picton, D. W. H. Rankin and H. E. Robertson, *Inorg. Chem.*, in the press; (e) D. Hnyk, P. T. Brain, H. E. Robertson, D. W. H. Rankin, M. Hofmann, P. v. R. Schleyer and M. Bühl, *J. Chem. Soc., Dalton Trans.*, 1994, 2885; (f) D. Hnyk, D. W. H. Rankin, H. E. Robertson, M. Hofmann, P. v. R. Schleyer and M. Bühl, *Inorg. Chem.*, 1994, **33**, 4781.

9 For example, see *Stereochemical Applications of Gas-Phase Electron Diffraction*, eds. I. Hargittai and M. Hargittai, VCH, Weinheim, 1990, Part A, p. 301; D. Hnyk, M. Bühl, P. v. R. Schleyer, H. V. Volden, S. Gundersen, J. Müller and P. Paetzold, *Inorg. Chem.*, 1993, **32**, 2442.

10 C. M. Huntley, G. S. Laurenson and D. W. H. Rankin, *J. Chem. Soc., Dalton Trans.*, 1980, 954.

11 C. R. Pulham, A. J. Downs, M. J. Goode, D. W. H. Rankin and H. E. Robertson, *J. Am. Chem. Soc.*, 1991, **113**, 5149.

12 S. Cradock, J. Koprowski and D. W. H. Rankin, *J. Mol. Struct.*, 1981, **77**, 113.

13 A. S. F. Boyd, G. S. Laurenson and D. W. H. Rankin, *J. Mol. Struct.*, 1981, **71**, 217.

14 A. W. Ross, M. Fink and R. Hilderbrandt, *International Tables for Crystallography*, ed. A. J. C. Wilson, Kluwer, Dordrecht, Boston and London, 1992, vol. C, p. 245.

15 GAUSSIAN 92, M. J. Frisch, G. W. Trucks, M. Head-Gordon, P. M. W. Gill, M. W. Wong, J. B. Foresman, H. B. Schlegal, K. Raghavachari, M. A. Robb, E. S. Replogle, R. Gomperts, J. L. Andres, J. S. Binkley, C. Gonzalez, R. Martin, D. J. Fox, D. J. DeFrees, J. Baker, J. J. P. Stewart and J. A. Pople, Gaussian Inc., Pittsburgh, PA, 1992.

16 CADPAC5: The Cambridge Analytical Derivatives Package, Issue 5. A suite of quantum-chemistry programs developed by R. D. Amos with contributions from I. L. Alberts, J. S. Andrews, S. M. Colwell, N. C. Handy, D. Jayatilaka, P. J. Knowles, R. Kobayashi, N. Koga, K. E. Laidig, P. E. Maslen, C. W. Murray, J. E. Rice, J. Sanz, E. D. Simandiras, A. J. Stone and M.-D. Su, Cambridge University, 1992.

17 W. Hehre, L. Radom, P. v. R. Schleyer, and J. A. Pople, *Ab Initio Molecular Orbital Theory*, Wiley, New York, 1986; T. H. Dunning and P. J. Hay, *Modern Theoretical Chemistry*, ed. H. F. Schaefer, Plenum, New York, 1977, vol. 3, p. 1.

18 S. Huzinaga, *J. Chem. Phys.*, 1965, **42**, 1293; T. H. Dunning, *J. Chem Phys.*, 1970, **53**, 2823; 1971, **55**, 716. A. D. McLean and G. S. Chandler, *J. Chem. Phys.*, 1980, **72**, 5639.

19 (a) P. v. R. Schleyer, M. Bühl, U. Fleischer and W. Koch, *Inorg. Chem.*, 1990, **29**, 153; (b) M. Bühl and P. v. R. Schleyer, *Angew. Chem., Int. Ed. Engl.*, 1990, **29**, 886.

20 S. Huzinaga, *Approximate Atomic Wavefunctions*, University of Alberta, Edmonton, 1971.

21 L. Hedberg and I. M. Mills, *J. Mol. Spectrosc.*, 1993, **160**, 117.

22 W. C. Hamilton, *Acta Crystallogr.*, 1965, **18**, 502.

23 See, for example, I. Hargittai and M. Hargittai, *Molecular Structures and Energetics. II. Physical Measurements*, VCH, New York, 1988, p. 417.

24 See also M. L. McKee, *J. Phys. Chem.*, 1990, **94**, 435.

25 M. Bühl, J. Gauss, M. Hofmann and P. v. R. Schleyer, *J. Am. Chem. Soc.*, 1993, **115**, 12385.

26 R. Greatrex, N. N. Greenwood, D. W. H. Rankin and H. E. Robertson, *Polyhedron*, 1987, **6**, 1849.

27 S. Konaka, Y. Murata, K. Kuchitsu and Y. Morino, *Bull. Chem. Soc. Jpn.*, 1966, **39**, 1134.

28 R. R. Ryan and K. Hedberg, *J. Chem. Phys.*, 1969, **50**, 4986.

29 P. T. Brain, A. J. Downs, M. Fanfarillo, M. J. Goode, A. G. Massey, D. W. H. Rankin and H. E. Robertson, *J. Mol. Struct.*, 1989, **192**, 163.

30 J. J. Briguglio, P. J. Carroll, E. W. Corcoran, jun. and L. G. Sneddon, *Inorg. Chem.*, 1986, **25**, 4618.

31 M. Hofmann and P. v. R. Schleyer, unpublished work.

32 S. K. Boocock, N. N. Greenwood, J. D. Kennedy, W. S. McDonald and J. Staves, *J. Chem. Soc., Dalton Trans.*, 1980, 790.

33 W. R. Pretzer and R. W. Rudolph, *J. Chem. Soc., Chem. Commun.*, 1974, 629.

34 R. P. Micciche, J. S. Plotkin and L. G. Sneddon, *Inorg. Chem.*, 1983, **22**, 1765.

35 P. T. Brain, A. J. Downs, P. Maccallum, D. W. H. Rankin, H. E. Robertson and G. A. Forsyth, *J. Chem. Soc., Dalton Trans.*, 1991, 1195.